Marine Geology 443 (2022) 106696

Contents lists available at ScienceDirect

Marine Geology

journal homepage: www.elsevier.com/locate/margo

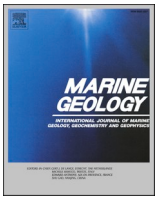

New insights on the Alboran Sea basin extension and continental collision from magnetic anomalies related to magmatism (western Mediterranean)

Víctor Tendero-Salmerón [a,*], Jesus Galindo-Zaldivar [a,b], Elia d'Acremont [c], Manuel Catalán [d], Yasmina M. Martos [e,f], Abdellah Ammar [g], Gemma Ercilla [h]

[a] Instituto Andaluz de Ciencias de la Tierra (CSIC-UGR), 18100 Armilla, Granada, Spain
[b] Departamento de Geodinámica, Universidad de Granada, 18071 Granada, Spain
[c] Sorbonne Université, CNRS-INSU, Institut des Sciences de la Terre Paris, ISTeP UMR 7193, 75252 Paris Cedex 05, France
[d] Royal Observatory of the Spanish Navy, 11100 San Fernando, Cádiz, Spain
[e] NASA Goddard Space Flight Center, Greenbelt, MD 20771, USA
[f] University of Maryland College Park, College Park, MD 20742, USA
[g] Faculté des Sciences, Université Mohammed V-Agdal, Rabat, Morocco
[h] Instituto de Ciencias del Mar, Continental Margins Group, CSIC, 08003 Barcelona, Spain

ARTICLE INFO

Keywords:
Magnetic anomalies
Igneous basic rocks
Rifting
Continental collision
Alboran Sea development

ABSTRACT

In the Alboran Sea there are a few well exposed Neogene and Quaternary volcanic zones, often geographic highs, that are generally associated with magnetic anomalies. In this paper, we present a characterization of these magnetic anomalies based on a recent and accurate magnetic data compilation for the Abloran Sea area. The anomalies reveal the distribution of magmatism and shed light into the discussion about the origin and evolution of the westernmost Mediterranean. One of the most relevant magnetic anomalies is the Nador dipole, which extends from the Gourougou volcano to the Chafarinas Islands, and is related to an *E*-W crustal scale intrusion. However, the main NE-SW elongated continuous dipoles of the central Alboran Sea are not related to any surface structure, but they are parallel to the Alboran Ridge, which is the main volcanic high in the Alboran Sea, and are located to the north of it. These anomalies extend discontinuously eastward along the NW-SE dipoles located along the Yusuf fault zone. The results of our 2D magnetic forward modeling suggest that the causative bodies of these main magnetic dipoles are deep igneous bodies. According to the tectonic evolution of the region, and the high magnetic susceptibility values obtained, these igneous bodies probably are made of a basic igneous rocks. Their emplacement may represent the westward tip of the rift axis of the AlKaPeCa Domain, which is related to the Oligocene-Miocene NW-SE extension, and associated with the southern slab retreat stage and oceanic spreading of the Algerian basin. Afterwards, these bodies were displaced toward the west, together with the Alboran Domain, and affected by the STEP fault located at its southern limit. Since the Late Miocene, the north Alboran Ridge elongated intrusions acted as a backstop that conditioned the folding and uplift of the Alboran Ridge in a tectonic indentation setting. In this setting, the STEP fault is deformed and the eastern part of the bodies were segmented along the Yusuf transtensional fault system. Simultaneously, the *E*-W crustal body related to the Nador magnetic dipole was emplaced, possibly evidencing a slab tearing process. The deep seated basic igneous bodies constitute main crustal heterogeneities that reveal and drive the Alboran Sea tectonic inversion.

1. Introduction

Back-arc basins are extensional structures formed in active continental margins generally related to oceanic lithosphere subduction (Taylor, 2013 and references therein). Extension in these basins is the consequence of a slab rollback (Heuret and Lallemand, 2005 and references therein). The rifting and magmatism associated to the spreading of back-arc basins may lead to the emplacement of igneous bodies that may be characterized by magnetic anomalies (Bohoyo et al., 2002; Catalán et al., 2013; Lawver and Hawkins, 1978; Taylor et al., 1996;

* Corresponding author.
E-mail addresses: vtendero@ugr.es (V. Tendero-Salmerón), jgalindo@ugr.es (J. Galindo-Zaldivar), elia.dacremont@sorbonne-universite.fr (E. d'Acremont), mcatalan@roa.es (M. Catalán), yasmina.martos@nasa.gov (Y.M. Martos), gemma@icm.csic.es (G. Ercilla).

https://doi.org/10.1016/j.margeo.2021.106696
Received 14 August 2021; Received in revised form 2 November 2021; Accepted 4 November 2021
Available online 14 November 2021

Weissel, 1981). Therefore, an analysis of the igneous bodies based on magnetic studies can provide clues for decoding the onset and evolution of back-arc basins.

The Western Mediterranean is a relevant area of back-arc basin occurrence, due to the slab rollback of the subducting African plate, which started during the Oligocene, and resulted in the extension and fragmentation of the southwestern margin of Europe (Doglioni, 1991; Gueguen et al., 1997, 1998; Malinverno and Ryan, 1986; Royden, 1993; Schettino and Turco, 2011; Spakman et al., 2018; Spakman and Wortel, 2004). The migration of arcs and collision with the nearby continental margins led to the formation of arc-shaped alpine orogens (Fig. 1a) and the extension in the fore-arc and back-arc basins, which ultimately underwent tectonic inversion (Faccena et al., 2014; de la Gómez Peña et al., 2020b; Yelles et al., 2009; and references therein). This is the case of the Gibraltar Arc, formed by the Betic and Rif Cordilleras, which encircles the Alboran Sea (Fig. 1, Comas et al., 1992; Corsini et al., 2014). The Internal Zones of the Gibraltar Arc (both those of the Rif and Betic Cordilleras) and the basement of the Alboran Sea basin constitute the Alboran Domain (Fig. 1b).

Two main groups of hypotheses have been proposed to explain the origin of the Alboran Domain extension. On one side, the lithospheric delamination hypotheses (e.g., Baratin et al., 2016; Mancilla et al., 2013; Seber et al., 1996; Valera et al., 2008), and on the other the subduction with slab rollback starting from the Miocene (e.g. Blanco and Spakman, 1993; Gutscher et al., 2012; Spakman et al., 2018; Fig. 1a). Tomographic results support a subduction system that is related to the Gibraltar Arc (Garcia-Castellanos and Villaseñor, 2011; Spakman and Wortel, 2004) more in accordance with the model of slab rollback and lithospheric tearing at the edges (e.g., Chertova et al., 2014; Faccena et al., 2014). Several paleogeographic reconstructions propose two consecutive stages of slab retreat since the Oligocene (e.g. Driussi et al., 2015). The first one is a south-eastern slab retreat that would have led to the displacement and initial extension of the Alboran Domain, as well as to the opening of the Algerian basin as a back-arc process (Gueguen et al., 1997; Mauffret et al., 2007; Romagny et al., 2020; Schettino and Turco, 2011; Spakman et al., 2018; Fig. 1a). The second one is a westward slab retreat that would have resulted in the migration of the Alboran Domain, thus causing the fore-arc and back-arc extension during the Miocene (Comas et al., 1999; Chertova et al., 2014; Gutscher et al., 2012; Schettino and Turco, 2011).

In this paper, a new case study based on magnetic anomaly data is presented, which improves the understanding of the geodynamic scenario of the Alboran Sea basin. This was possible through the use of a recent magnetic data compilation for the study of the main magnetic anomalies produced by major igneous crustal bodies. Their structure and significance, in the context of the back-arc rifting, were analyzed in

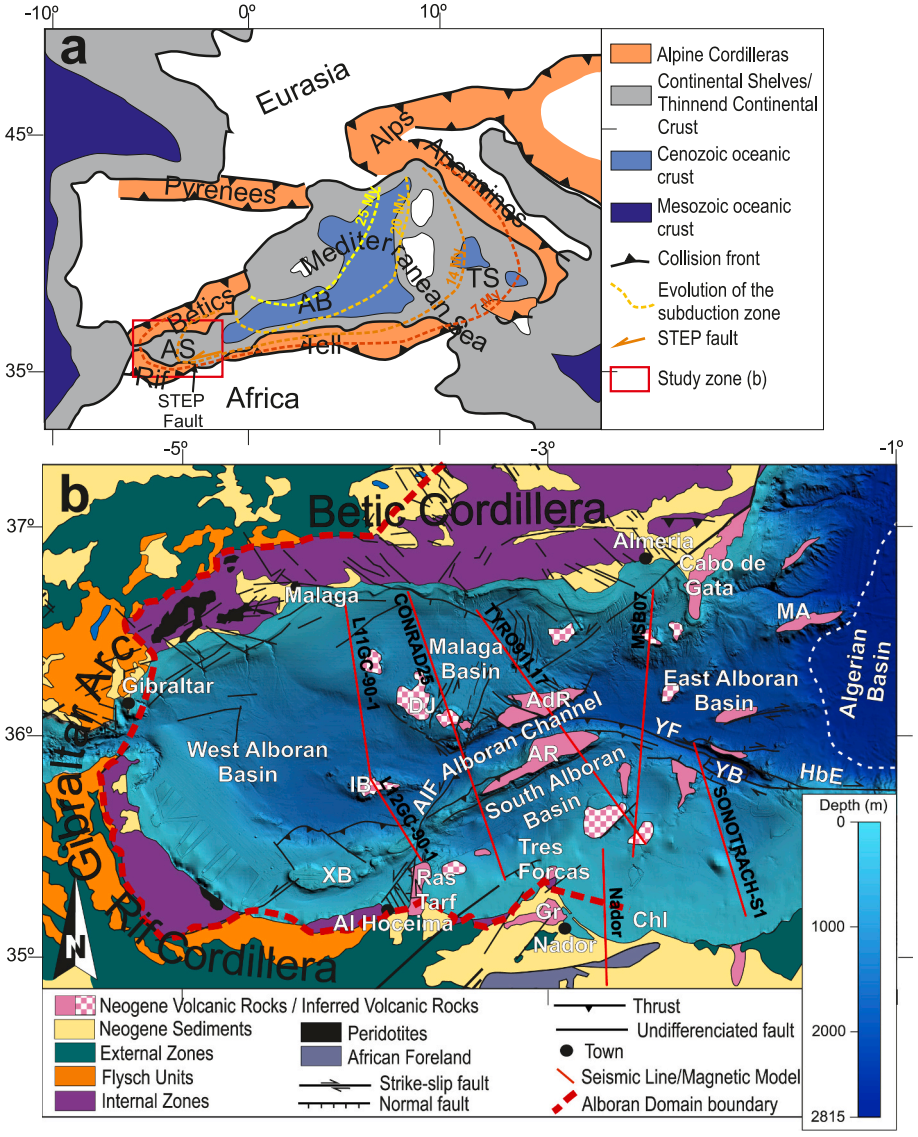

Fig. 1. Geological context of the study zone. a. Tectonic sketch of the western Mediterranean Sea based on Do Couto et al. (2016) that includes the evolution of the subduction zone associated to the opening of the Western Mediterranean (d'Acremont et al., 2020; Do Couto et al., 2016; Faccena et al., 2014; Rosenbaum et al., 2002). AB: Algerian basin, AS: Alboran Sea. b. Simplified geological map of the Alboran Sea based on Hidas et al. (2019) and d'Acremont et al. (2020). The inferred volcanic rocks correspond to outcrops where there are no dredged or drilled samples to confirm them. The paths of the seismic profiles used to constrain the forward models of magnetic anomalies are included. The approximated boundaries of Alboran Domain are depicted. Eastern boundary is still discussed, so it is not depicted. AIF: Al Idrissi Fault, AR: Alboran Ridge; AdR: Adra Ridge, ChI: Chafarinas Islands, DJ: Djibouti Bank, GR: Gourougou volcano, HbE: Habibas Escarpment, IB: Ibn-Batouta Bank, MA: Maimonides High, XB: Xauen Bank, YB: Yusuf Basin, YF: Yusuf Fault.

order to reveal new clues on the extensional deformations that created the Alboran Sea basin, as well as the development of the STEP fault (Subduction Tear Edge Propagator fault, Govers and Wortel, 2005), and the recent tectonic indentation. This contribution also highlights the impact that large igneous bodies intruded during the initial continental rifting stages had on the sedimentary basin evolution.

2. Regional setting

The Alboran Sea basin is located in the westernmost part of the Mediterranean. It is bounded by the Gibraltar Arc (Betic and Rif cordilleras, Fig. 1). The basin can be subdivided into four sub-basins separated by the main highs, which are the West Alboran Basin (the largest one), the Eastern Alboran Basin (which is opened to the Algerian Basin), the South Alboran basin and the Malaga Basin (Fig. 1b). The basement is formed by asymmetric thinned continental crust evidenced by deep seismic profiles (de la Gómez Peña et al., 2020a; Suriñach and Vegas, 1993), reaching 16 km of thickness from the northern margin to the Alboran Ridge, and progressively thickening southwards up to more than 30 km under the Rif. Seismic refraction profiles and potential field data indicate that the mantle below the Alboran Sea basin is low density and low P-velocity anomalous (Galindo-Zaldivar et al., 1998; Hatzfeld, 1976; Suriñach and Vegas, 1993). The Alboran Sea basin opens eastwards to the oceanic Algerian basin (e.g., Faccena et al., 2014; Gueguen et al., 1997). The thinned continental crust basement, which constitutes the Alboran Domain, is represented by alpine metamorphic rocks (mainly metapelites) of the Internal Zones of the Betic and Rif cordilleras (Comas et al., 1992; García-Dueñas et al., 1992) that include peridotites (Garrido, 1995). Although the Alboran Sea is considered a current back-arc basin associated to a westward subduction (e.g., Balanya et al., 2012; Chertova et al., 2014; Comas et al., 1999; González-Castillo et al., 2015a; Gutscher et al., 2012), recent studies propose an alternative subdivision into three crustal domains: i) the West Alboran and Malaga basins together representing a Miocene fore-arc basin; ii) the East Alboran Basin, the Alboran Ridge and the Alboran Channel, forming part of a magmatic arc; and iii) the area located southwards of the Yusuf fault and the Alboran Ridge, which is considered part of the African margin (Booth-Rea et al., 2007; d'Acremont et al., 2020; de la Gómez Peña et al., 2020a; de la Gómez Peña et al., 2020b). The sedimentary infill is Miocene (Aquitanian-Burdigalian) to Quaternary in age and mainly detritic (Comas et al., 1992; Juan et al., 2016).

The geological evolution of the Alboran Domain is the consequence of the motion and rifting of the AlKaPeCa Domain (Bouillin et al., 1986) between the Eurasian and African plates, started in the Late Oligocene-Miocene (Chertova et al., 2014; Comas et al., 1999; Mauffret et al., 2007; Romagny et al., 2020; Rosenbaum et al., 2002). The AlKaPeCa Domain is described as a landmass that, before the Miocene, was part of the fore-arc and accretionary prism that originally formed on the Eurasian side of the African-Eurasian collision (Bouillin et al., 1986). Its name refers to the domains that were formed by its fragmentation (Bouillin et al., 1986): the Alboran Domain, the Kabyiles (Argelia), the Peloritan Range (Sicily) and Calabria (South Italy). The AlKaPeCa Domain experienced at least 200 km of roughly N-S extension (or even more, Faccena et al., 2014), which started during the Late Oligocene (27–25 Myr) and was related to the southward retreat of the slab. This N-S to NW-SE extension was characterized by a top-to-the north detachment (Jolivet et al., 2021 and references therein) and led to the beginning of the oceanic spreading of the Algerian basin during the Early Miocene (Faccena et al., 2014; Romagny et al., 2020; Rosenbaum et al., 2002; Schettino and Turco, 2011; Driussi et al., 2015). After the opening of the Algerian basin, the extension changed direction to *E*-W, in relation to a westward Gibraltar slab retreat and, therefore, to a westward motion of the Alboran Domain. During the Miocene, the westward displacement of the subduction zone has been accommodated by a STEP (Subduction Tear Edge Propagator) fault in the southern limit of the Alboran Domain (e.g. d'Acremont et al., 2020). STEP faults are subvertical, lithospheric-scale tear faults located at the edges of a segmented slab (Govers and Wortel, 2005).

The extension of the Alboran Domain was followed by compression since the Late Tortonian (Comas et al., 1999; Do Couto et al., 2016), when the westward retreat of the Gibraltar slab decreased (d'Acremont et al., 2020). The NW-SE oblique Eurasian-Africa plate convergence was combined with the orthogonal extension associated to the westward motion of the Alboran Domain (Comas et al., 1992; Corsini et al., 2014; DeMets et al., 2010; González-Castillo et al., 2015a; Neres et al., 2016; Watts et al., 1993). Strike-slip faulting has affected the central Alboran Sea since the Late Miocene, forming the main NW-SE dextral and NE-SW sinistral fault sets that cross the basin and continue up to the coast (Fig. 1b). Two of the most relevant strike-slip faults of these sets are the Al Idrissi and the Yusuf faults (Fig. 1b). While the Al Idrissi fault zone has been considered to be a Pleistocene structure (Lafosse et al., 2020), the Yusuf fault is interpreted as being older, inherited from the STEP fault that accommodated the westward displacement of the Alboran Domain, and deformed by the compression (d'Acremont et al., 2020). The Yusuf fault presents a complex structure with related folds and basins, divided into two segments by the Habibas Escarpment (Fig. 1b, Martínez-García et al., 2011). The fault is also considered to be a main contact between the thinned continental crust of the African plate and both the magmatic thinned crust of the East Alboran Basin, and the oceanic crust of the Algerian Basin (Booth-Rea et al., 2007; de la Gómez Peña et al., 2020a; Suriñach and Vegas, 1993). The Al Idrissi and Yusuf faults have been interpreted as being part of a tectonic indentation structure that affects the Central Alboran Sea and causes the elevation of the Alboran Ridge (Estrada et al., 2018; Lafosse et al., 2020). According to this model, the Alboran Ridge uplift above the Alboran Channel would be the consequence of the NNW directed collision of the rigid basement block of the southern part of the Alboran Sea basin, bounded by the Al Idrissi and the Yusuf faults (Fig. 1b, Estrada et al., 2018).

2.1. Magmatism

From the Miocene to the Pleistocene, magmatism affected the Alboran Domain due to lithospheric thinning and the related increase in the geothermal gradient (which continues being high, at least in the eastern part) (Fig. 1, Andrés et al., 2018; Comas et al., 1992, 1999; Davies, 2013; Duggen et al., 2008; Polyak et al., 1996). Most of the highs, seamounts and ridges of the Alboran Sea have been considered volcanic outcrops (e.g., Booth-Rea et al., 2007; Comas et al., 1999), mainly made up of basic or intermediate rocks (basalt and andesites, e.g., Duggen et al., 2008; Fernández-Soler et al., 2000). Geochemical studies show a zonation of the magmatism characterized by tholeiitic, calc-alkaline and shoshonitic series (Middle Miocene to Early Pliocene), which are believed to be of volcanic arc type, present in the central and eastern Alboran Sea; while basanites and alkali basalts (Late Miocene to Pleistocene) appear in the eastern onshore Alboran Domain (Coulon et al., 2002; Duggen et al., 2004, 2008; Fernández-Soler et al., 2000; Gill et al., 2004; Hoernle et al., 1999). Three main hypotheses can explain the geochemical affinity of the Alboran magmatism (Duggen et al., 2008): a) MORB-type parental magmas with significant crustal contamination, which generate calc-alkaline lavas similar to subduction-related ones (Turner et al., 1999); b) crustal sources without mantle implication (Zeck et al., 1998); and c) tholeiitic and calc-alkaline series from a subduction-modified mantle with different degrees of crustal contamination (Coulon et al., 2002; Hoernle et al., 1999). The last stages of volcanism (basanites, alkali basalts, hawaiites and tephrites of Late Miocene to Pliocene age) occur offshore in eastern Morocco, northern Algeria and SE Spain, and are related to intraplate post-collisional magmatism (Duggen et al., 2005). Some of these volcanic zones include rocks of both stages (the calk-alkaline and shoshonitic stage and the late, alkaline stage), such as the Gourougou volcano (Fig. 1, El Bakkali et al., 1998). The occurrence of this volcano has been related to a tearing of the oceanic slab attached to the African margin

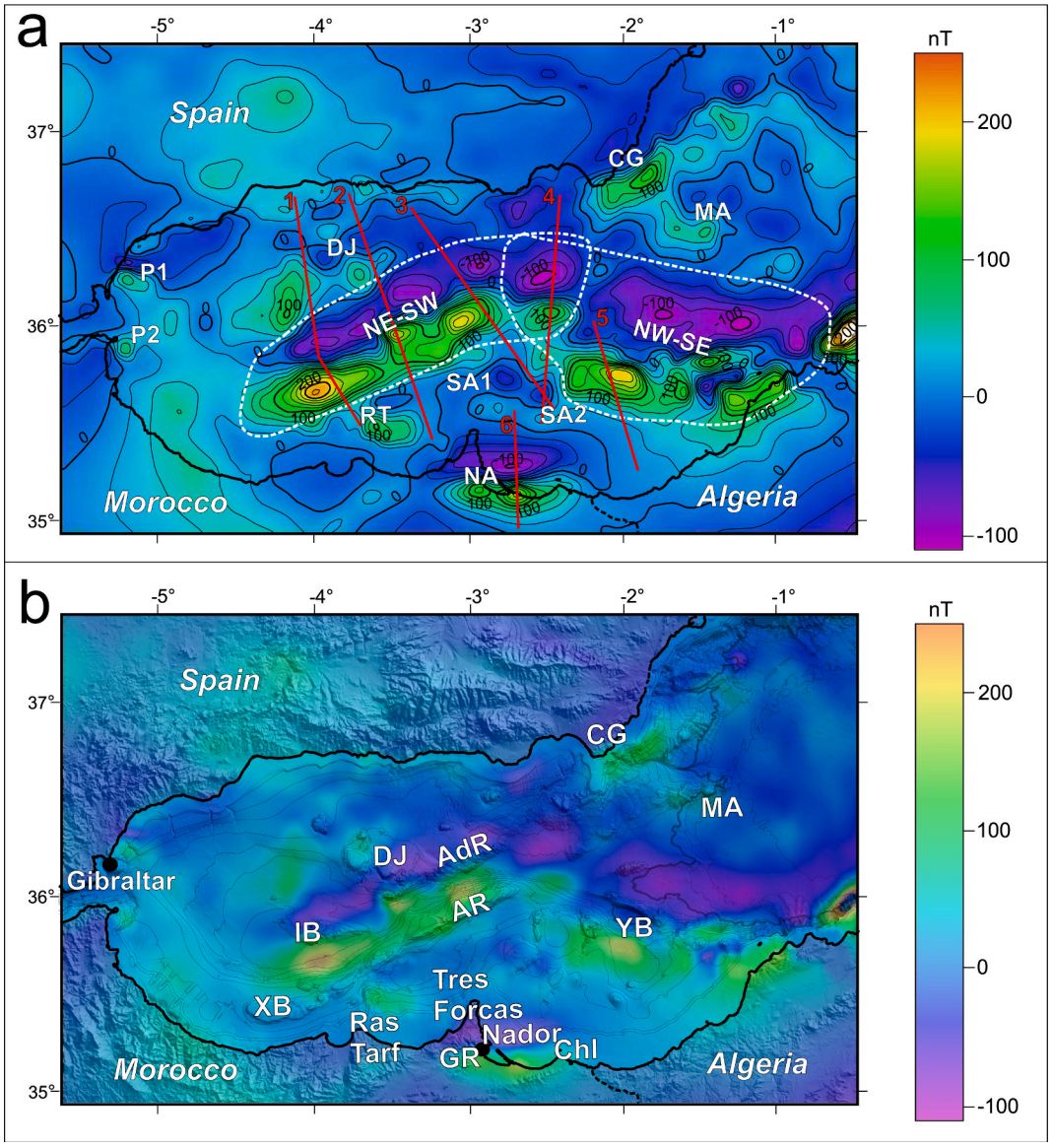

Fig. 2. Magnetic anomaly maps of the Alboran Sea. a. Magnetic anomaly map of the Alboran Sea at 3 nautical miles resolution. Minor contour lines every 20 nT and major every 100 nT. The paths of the profiles are depicted and numbered as follows: 1. L12GC-90-1- L11GC-90-1, 2. CONRAD825, 3. TYRO91L17, 4. MSB07, 5. SONOTRACH_S1 and 6. Nador. The white abbreviations are the names given to the dipoles (further description in sections 4 and 5). The NE-SW and NW-SE dipole lineations are circled with a dashed line. b. Magnetic anomaly map superimposed over a relief map of the Alboran Sea with bathymetry contour lines every 200 m and the coast line in black. AR: Alboran Ridge, AdR: Adra Ridge, ChI: Chafarinas Islands, GR: Gourougou volcano, IB: Ibn-Batouta Bank, XB: Xauen Bank, YB: Yusuf Basin

(Carminati et al., 1998; Duggen et al., 2005; Hidas et al., 2019; Jolivet et al., 2021; Maury et al., 2000).

The magnetic anomalies of the Alboran Sea have been associated with basic igneous rocks since the publication of the aeromagnetic map presented by Galdeano et al. (1974). One of the most important anomalies is that of Nador (Figs. 1 and 2), which was constrained from onshore field observations (Anahnah et al., 2009) and that continues offshore. In the central basin, Galindo-Zaldivar et al. (1998) suggested that the Alboran Ridge is not the causative body of the main observed magnetic dipoles, even though the Alboran Ridge is considered to be made of volcanic rocks (e.g. Booth-Rea et al., 2007). The magnetic models provided in this study improved the modeling made by Galindo-Zaldivar et al. (1998) and support the presence of deep igneous bodies as origin of those magnetic dipoles, although the models are open to alternative interpretations.

3. Materials and methods

3.1. Magnetic anomaly analysis

To produce the magnetic anomaly map presented with this work we used data from the second version of the World Digital Magnetic Anomaly Map Project (http://wdmam.org/). This worldwide map has a 3 nautical miles resolution. The data were gathered at a variety of altitudes, but normalized at 5 km above sea level on the continents, and at sea level for marine surveys (Catalán et al., 2016: Lesur et al., 2016). The map of the Alboran Sea area has been obtained by combining different line orientations, mainly *E*-W, NW-SE and NE-SW, with a line spacing smaller than 20 km in most of the zones. This map is suitable for studying magnetic anomalous bodies whose size ranges from several to tens of kilometers, without noise originated by small, shallow bodies. It encompasses data from different international sources whose acquisition times span from 1964 until 2016. The way these data were

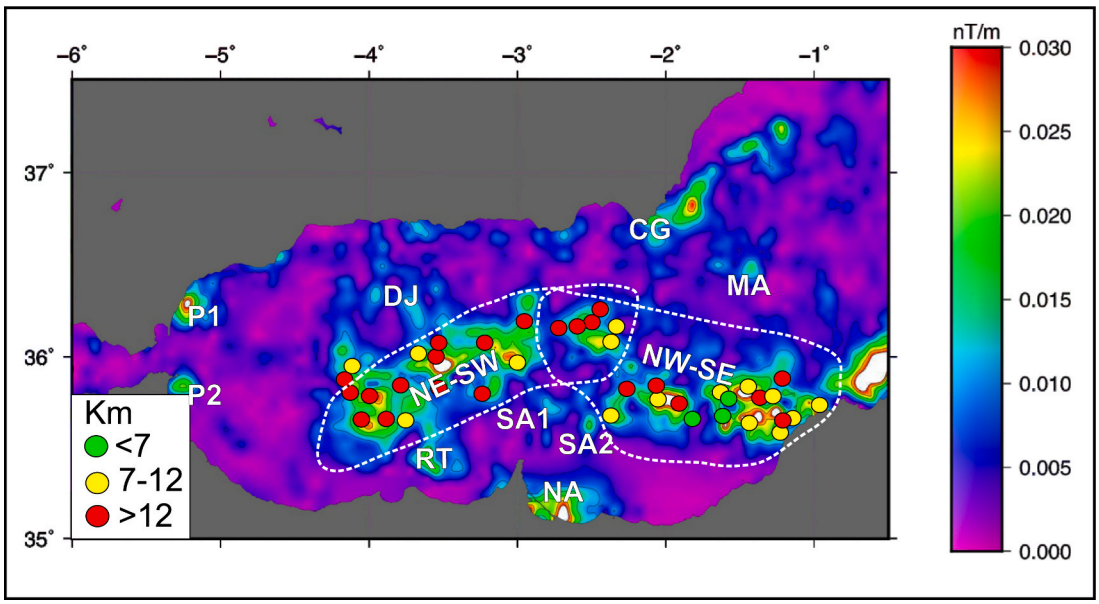

Fig. 3. Analytical signal map of the Alboran Basin with the depth Euler solutions in km. The names of the corresponding magnetic anomalies are depicted. The white abbreviations are the names given to the dipoles (further description in sections 4 and 5).

processed to improve their internal coherency is described in Quesnel et al. (2009) and Lesur et al. (2016).

After obtaining the magnetic anomaly map (Fig. 2), the analytic signal (AS, Fig. 3) was calculated. This is defined as the square root of the squared sum of the vertical and two orthogonal horizontal derivatives of the magnetic field anomaly (Nabighian, 1984; Roest et al., 1992; Roest and Pilkington, 1993; Salem et al., 2002):

$$|AS(x,y,z)| = \sqrt{\left(\frac{\partial M}{\partial x}\right)^2 + \left(\frac{\partial M}{\partial y}\right)^2 + \left(\frac{\partial M}{\partial z}\right)^2} \quad (1)$$

where $|AS(x,y,z)|$ is the amplitude of the AS, and M the magnetic anomaly intensity.

Therefore, the resulting 3D AS map summarizes the net variation of the gradient of the magnetic anomaly field intensity in 3D. One of the most attractive aspects of this 3D operator is the fact that its amplitude produces maximum amplitude along the lateral edges of the causative body, regardless of the direction of magnetization, or its induced and/or remanent character (Keating and Sailhac, 2004; Roest et al., 1992; Roest and Pilkington, 1993). In this sense, there is no need to assume a purely induced magnetization effect hypothesis or to discuss possible remanent vector space orientation. Such a simplistic approach (a purely induced magnetization effect hypothesis) could lead to severe distortion in environments where remanent effects play an important role.

Magnetic techniques were used in order to identify deep structures. To this end, an algorithm based on the Euler deconvolution was applied to estimate the depth to the top of the different magnetic horizons. This procedure was performed by selecting a square window of data from a total field grid and its orthogonal derivatives. Euler's equation was solved using the least squares method, simultaneously for each grid position, within every window (Ravat, 1996; Reid et al., 1990; Thomson, 1982). The equation includes the degree of homogeneity, "N", which usually refers to the structural index (S.I.). This index is a measure of the rate of change with distance of a field.

$$(x-x_0)\frac{\partial M}{\partial x} + (y-y_0)\frac{\partial M}{\partial y} + (z-z_0)\frac{\partial M}{\partial z} = NM \quad (2)$$

where M is the magnetic anomaly intensity at location (x, y, z), caused by a magnetic source at location (x_0,y_0,z_0), and N denotes the structural index.

The results of the Euler deconvolution and the Curie point depth have been used to constrain the maximum depth where the anomalous magnetic bodies may be located. The AS depths (Fig. 3) were obtained using the so-called "Standard Euler Deconvolution". This procedure was performed by selecting a square window of data from a total field grid and its orthogonal derivatives. Euler's equation was solved using the least squares method, simultaneously for each grid position, within every window. A value of 2 was used as Structural Index (SI). An index of 2 indicates a body with one infinite dimension. That value was chosen because, in our opinion, it is the option that best represents the geometries of the NE-SW and NW-SE magnetic anomalies: a limited depth and width, with the longest dimension extending along the Alboran Basin. The accepted solutions were only those with a depth tolerance smaller or equal to 15%. A value of 26 km was set as window size, which is the width of the anomalies (according to the AS map) that we are interested in the Alboran ridge and the Yusuf fault zone.

Furthermore, it is necessary to consider the Curie point depth, or Curie depth, the depth at which magnetic minerals lose their magnetic properties due to temperature. Several factors, such as composition variability, could result in uncertainties in the estimation of the Curie depth. For this reason, causative bodies, in order to be safely considered as such, must be emplaced a few kilometers over the Curie depth of the region. These data were obtained from Li et al. (2017). It is also important to note that both depths, the Curie depth and the Euler deconvolution depths, are used initially as guiding depths to localize the causative bodies for the forward modeling.

The 2-D forward modeling of the magnetic anomalies (Figs. 5, 6 and 7) was obtained using the GravMag 1.7 software of the British Geological Survey (Pedley et al., 1993). The magnetic susceptibility values of the anomalous magnetic bodies are based on those used in Galindo-Zaldivar et al. (1998). Three types of bodies were considered (Fig. 5): those with high susceptibility (0.07 SI, basic or intermediate igneous rocks, in black); those with medium values of susceptibility (0.02 to 0.045 SI, areas where there is a mixing of metamorphic and igneous rocks, marked in brown and green); and those with very low susceptibility (< 0.02 SI, sediments and the rest of the basement host rock, respectively marked in yellow and beige). Moreover, for the causative bodies of the major dipoles (bodies in black), which are the main target of the models, three values of susceptibility (0.05, 0.07 and 0.10 SI) have been considered. This way, the effect of susceptibility on the geometry

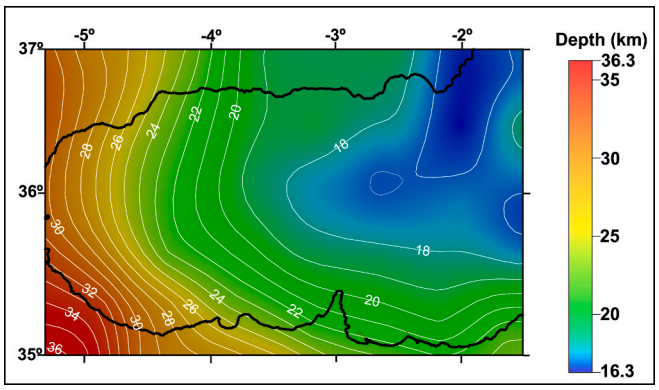

Fig. 4. Curie depth map for the Alboran Sea based on Li et al. (2017) data. Contour lines every 1 km.

and depth of the bodies was tested.

The appearance of the magnetic anomalies in the Alboran Sea consists of dipoles that show highs to the south and lows to the north (Fig. 2). This polarity is compatible with the induced magnetic anomalies produced by the current Earth's magnetic field in the northern hemisphere (e.g., Telford et al., 1990). Consequently, in the absence of direct information on the remanent magnetization, it was decided not to separate the remanent from induced magnetic contributions in our forward modeling, similarly to what Galindo-Zaldivar et al. (1998) did. The susceptibilities should be interpreted as apparent values. The magnetic dipoles that have been modeled are those that present amplitudes >200 nT, which are also tens to hundreds of kilometers long. The dipoles are considered when magnetic highs and lows with similar size are aligned in a direction close to N-S. During the modeling, as previously mentioned, the deepest anomalous bodies that have been considered were positioned at least a few kilometers over the Curie depth, to avoid possible demagnetization due to high temperatures close to this boundary (Fig. 4). The depths obtained from the Euler deconvolution (Fig. 3) were used as a guideline during the modeling.

In addition, seven multichannel seismic reflection profiles from the database of the Instituto de Ciencias del Mar (ICM-CSIC http://www.

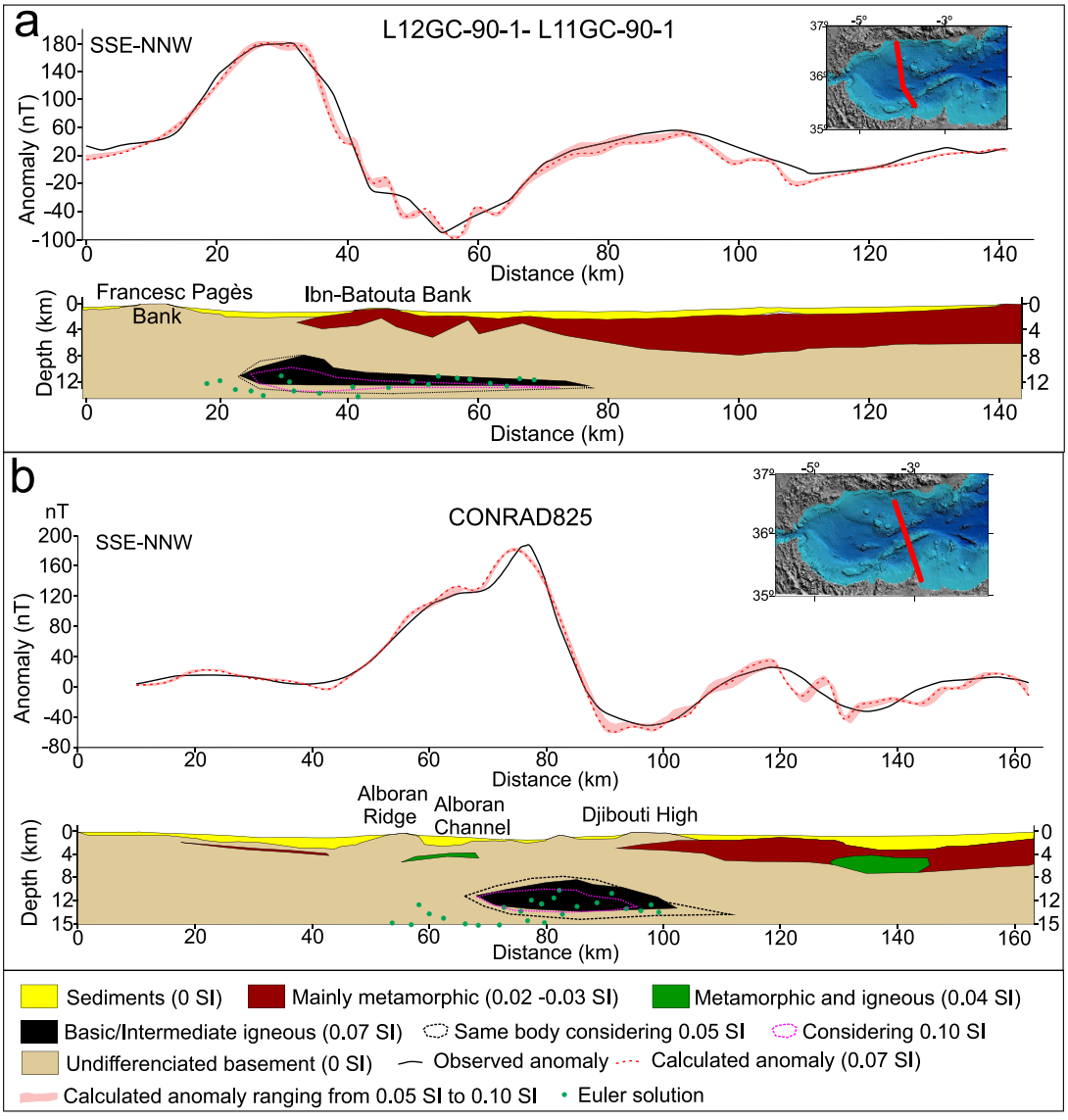

Fig. 5. Magnetic anomaly profiles and forward models of the NE-SW dipole lineation (L12GC-90-1- L11GC-90-1 and CONRAD825). The inset in the upper right corner shows the position of the profile in the Alboran Sea.

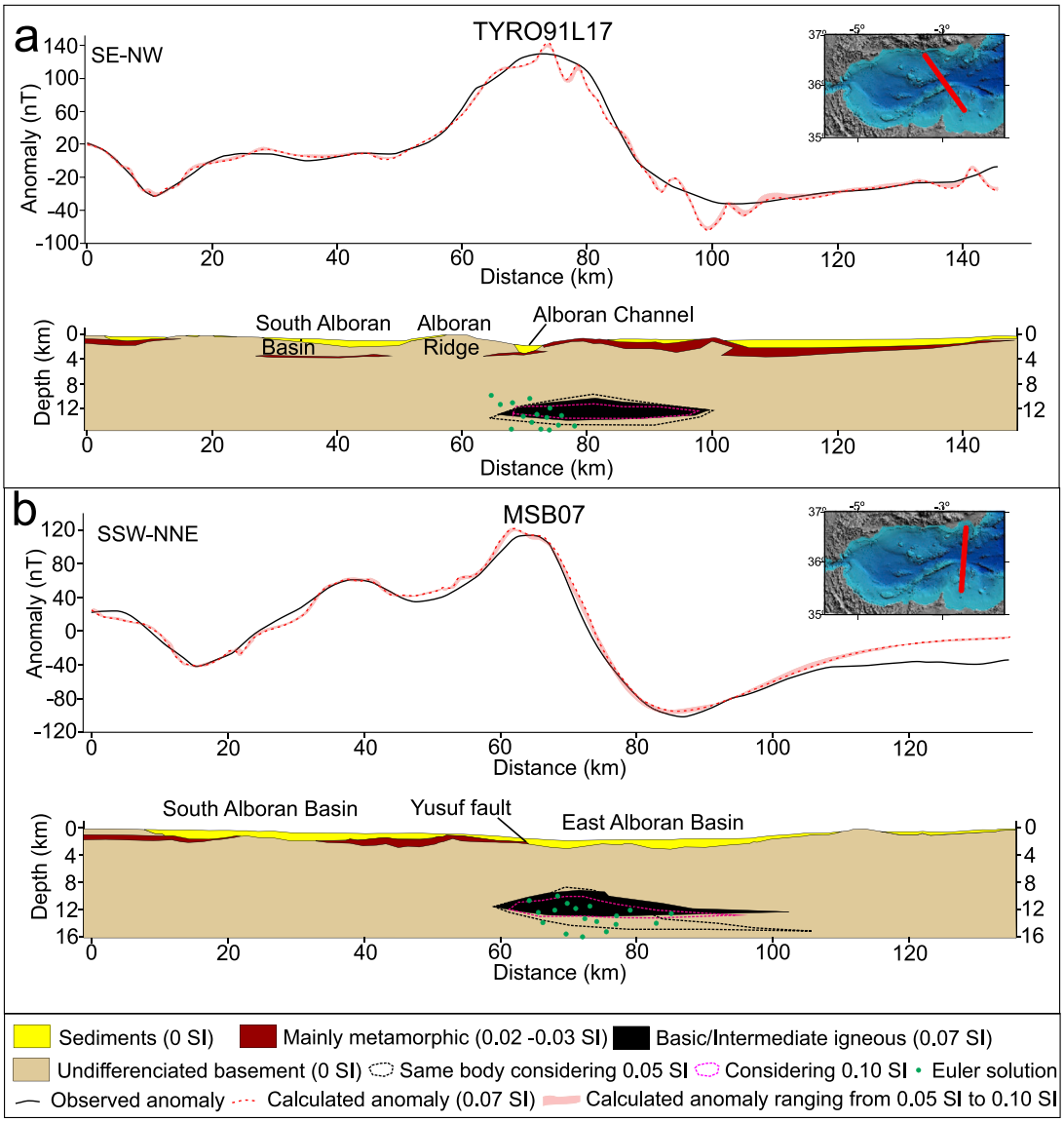

Fig. 6. Magnetic anomaly profiles and forward models of the NE-SW dipole lineation (TYRO91L17) and of the area where the NE-SW and NW-SE lineations cross (MSB07). Insets in the upper right corner show the position of the profiles in the Alboran Sea.

icm.csic.es/geo/gma/SurveyMaps, Figs. 1 and 5) were selected and analyzed in order to (i) check that the magnetic anomalous bodies were not intruded into the sedimentary infill, and (ii) determine the basement-sediments contact location. These profiles, which have been realized following standard procedures of acquisition and processing, were selected on the basis of their location and position orthogonal to the main dipoles (see Supplementary Files). The profiles L12GC-90-1 and L11GC-90-1 are joined (Fig. 6). Only the model of the Nador dipole (Figs. 2, NA, and 7) is not based on a seismic line, because of the lack of seismic profiles.

4. Results

4.1. Magnetic anomalies and igneous rocks

This study is focused on the magnetic dipoles of kilometric scale that appear in the Alboran Sea. In order to describe them, two main groups can be considered: dipoles related to the Late Miocene to Pliocene volcanic seafloor outcrops, and those without an apparent link with mapped igneous rocks. The first group of dipoles includes the dipoles CG (Cabo de Gata), DJ (Djibouti Bank), MA (Maimonides High), NA (Nador), RT (Ras Tarf), SA1 and SA2 (South Alboran 1 and 2, Fig. 2a). CG is NE-SW elongated and is found close to the Cabo de Gata coast (Fig. 2, CG). This dipole has a high of 130 nT and a low of −40 nT, only partially identified offshore. This anomaly is related to the Cabo de Gata volcanic rocks (Fig. 1b). To the southeast of this dipole, another smaller dipole is found aligned with the Maimonides High, also of volcanic nature (Figs. 1b and 2, MA). This dipole ranges from −20 nT to 60 nT. The north-western part of the Alboran Basin is dominated by two elongated positive N-S anomalies (100 and 60 nT) near −4° of longitude. They are geographically correlated with the Djibouti Bank (Fig. 2, DJ).

On the other hand, the dipoles located in the southern Alboran Sea (RT, SA1, SA2 and NA, Fig. 2) are related to prolongations of the volcanic rocks outcropping at the coastal area. The RT dipole (Fig. 2), with a high over 100 nT and a low of −10 nT, is located at the northern prolongation of the volcanic Ras Tarf cape (Booth-Rea et al., 2007; Comas et al., 1999). SA1 and SA2 (with 30 nT in the highs and − 40 nT in the lows, Fig. 2) occur close to the Tres Forcas Cape Ridge, where the substrate is considered to be volcanic rocks (Fig. 1, Martínez-García et al., 2011). To the east of Nador (Figs. 1b and 2, NA), an *E*-W 60 km elongated magnetic anomaly dipole is related onshore to the Gourougou volcano, and extends eastwards offshore up to the Chafarinas volcanic

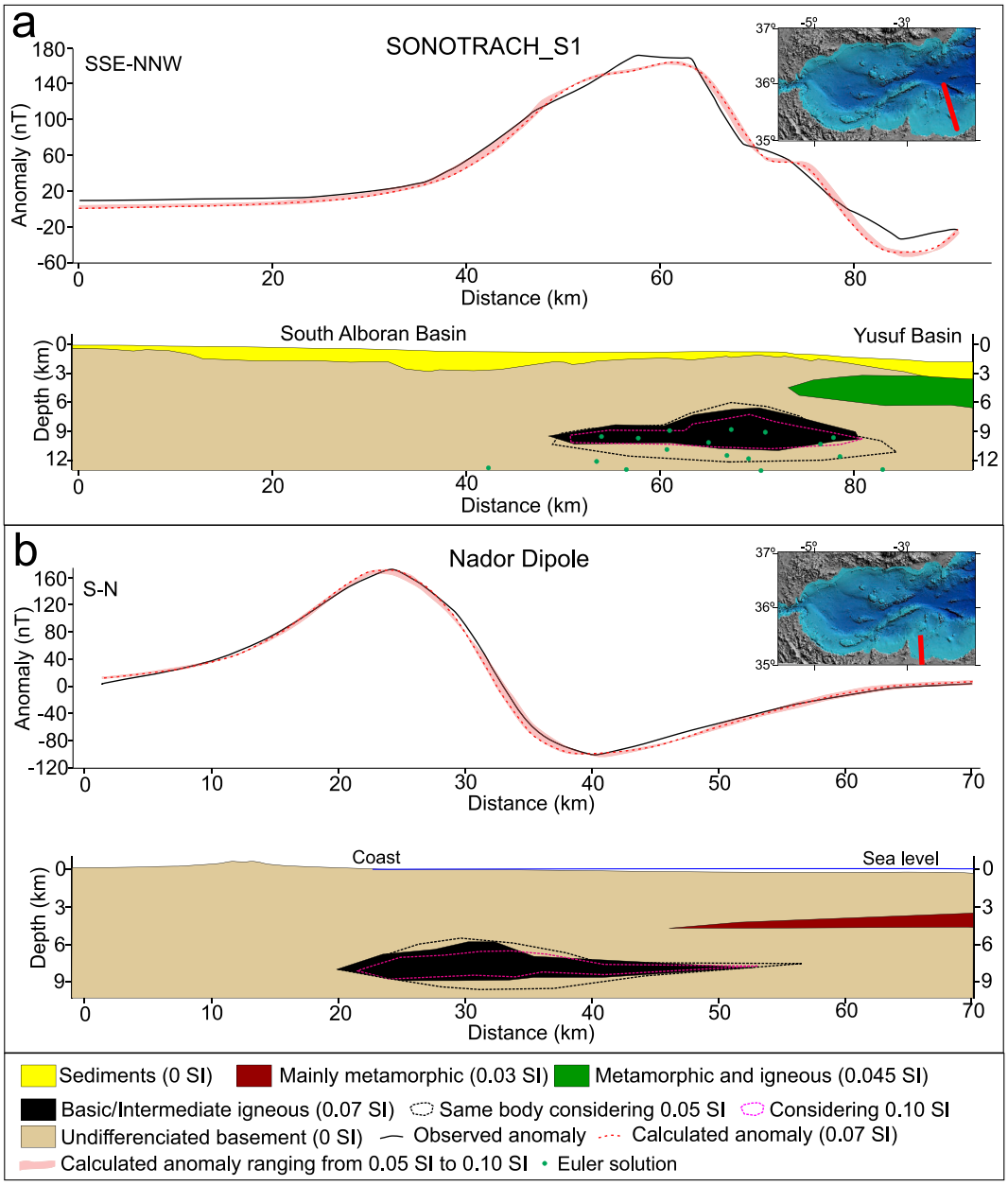

Fig. 7. Magnetic anomaly profiles and forward models of the NW-SE dipole (SONOTRACH_S1) and of the Nador dipole (Nador). Insets in the upper right corner show the position of the profiles in the Alboran Sea.

islands. This dipole has a high of 170 nT and a low of −100 nT, which puts it close to the highest amplitudes of the Alboran Sea (~270 nT, Figs. 2 and 7).

With regards to the group of dipoles that are not related with mapped igneous rocks, they comprise the NE-SW and NW-SE dipole lineations with relatively large scale and amplitude, and the P1 and P2 dipoles, which are smaller in scale and amplitude (Fig. 2, P1, P2 and NE-SW and NW-SE dipoles lineations). The NE-SW and NW-SE dipole lineations are parallel to the main structures of the central and eastern Alboran Sea, such as the Alboran Ridge, the Adra Ridge and the Yusuf fault zone (Figs. 1b and 2). These lineations intersect approximately at 2°30′ W in a dipole with values reaching −100 nT and 110 nT (Fig. 2). To the west, the NE-SW anomaly shows a continuous plot up to 4°30′W, in line with the western end of Ibn-Batouta bank. Its average intensity is 120 nT along its highs, reaching more than 200 nT at one location. The lows show values of −80 nT. This NE-SW lineation is located north of the Alboran Ridge and of the Xauen Bank (Figs. 1b and 2, Galdeano et al., 1974; Galindo-Zaldivar et al., 1998). To the east, the NW-SE dipole lineation presents similar values, although there are two significant differences: the geometry is more irregular and formed by different local dipoles, and the lows are generally wider than the highs, which reach up 170 nT (Fig. 2). Furthermore, the NW-SE anomaly changes its trend eastwards at 1°W, becoming parallel to the shoreline (Fig. 2), but keeping high amplitudes of more than 200 nT (highs over 140 nT and lows below −100 nT).

The small-scale dipoles P1 and P2, in the Westernmost Alboran Sea, north and south of the Strait of Gibraltar, are not even next to, or parallel to offshore structures. These two small and intense dipoles are located at both sides of the strait close to the coast, with highs of 70 nT (Fig. 2, P1) and 90 nT (Fig. 2, P2) and lows that reach −70 nT.

The analytic signal map and depth determinations of the magnetic anomalies of the Alboran Sea show the range of depth of the causative bodies for the NE-SW and NW-SE dipole lineations (Fig. 3). This depth ranges between <7 km and > 12 km along the NE-SW trending magnetic

anomaly (Fig. 3). 82% of the solutions are deeper than 12 km, and only 9% of them are deeper than 18.6 km. This means that a remarkable fraction of depth from the top lies between 12 km and 18.6 km. For the NW-SE trending magnetic anomaly, our solutions are shallower on average (11.9 km), but they are more scattered, covering a wide range of depths between 5 km to 15 km.

4.2. Forward modeling of magnetic anomalies

The Nador dipole (NA, Fig. 2a) and the NE-SW and NW-SE dipole lineations represent the main magnetic anomalies of the Alboran Sea, with amplitudes of ~200 nT or more (270 nT in the case of the Nador dipole). In order to quantitatively constrain the geometry and location of their causative bodies, six 2D forward models have been computed (Figs. 5, 6 and 7); five of them were constrained by seismic reflection profiles to determine the basement-sediments contact depth (see Supplementary Files). The Nador model was performed without determining the basement-sediments contact because no seismic profiles were available over the whole dipole (Fig. 7). The Nador model is located east of the Gourougou volcano and shows a 0.07 SI magnetic susceptibility body of roughly 35 km of width at 5–9 km of depth close to the coast (Fig. 7). This body should have an oval shape that wedges northwards. In the northern part of the profile there is a thin body of 0.03 SI magnetic susceptibility, with a 2 km thickness and located at 3.5 km of depth (Fig. 7).

Regarding the central and eastern Alboran sea areas, three models are focused on the NE-SW dipole lineation in the central Alboran Sea (Fig. 5: associated with the seismic profiles CONRAD825 and the L11–12GC model that joins profiles L11GC-90-1 and L12GC-90-1; Fig. 6: the profile TYRO91L17). The model of profile MSB07 is located in the corner of the NE-SW and NW-SE dipole lineations of the eastern Alboran Sea (Figs. 2a and 6), and lastly, the model of the profile SONOTRACH_S1 (Fig. 7) is focused on the NW-SE dipole lineation.

The NE-SW dipole lineation in the central Alboran Sea is related to a deep (8–14 km) body of 0.07 SI magnetic susceptibility (Figs. 3, 5, 6 and 8). In the southwestern end of this anomaly, the causative body extends to 8–13 km of depth, slightly south of the Ibn-Batouta Bank, with a thickness of 5 km in the southern part, thinning northwards and reaching almost 60 km of width (L11–12GC model, Fig. 5). From the Ibn-Batouta Bank northwards, a shallow crustal body of 0.03 SI magnetic susceptibility is needed to fit the anomaly. This body should be positioned below the sedimentary cover, and have a thickness that increases northwards up to 5 km. In the CONRAD825 model (Fig. 5) the deep body is 40 km wide, between the Djibouti High and the Alboran Channel, has a thickness of 6 km and is located at 6–14 km of depth. The shallow crustal body is shorter and thinner than in the L11–12GC model and includes a body of 0.04 SI magnetic susceptibility in the northern part (Fig. 5). Two more thin and shallow crustal bodies are needed: one of 0.04 SI magnetic susceptibility under the Alboran Channel, and one of 0.03 SI magnetic susceptibility to the south of the Alboran Ridge. The TYRO91L17 model shows again the main deep body located to the north of the Alboran Ridge, at 9–13 km of depth (Fig. 6). This body has a thickness of 4 km and is 40 km wide. The shallow crustal body of the northern half of the profile is thinner (maximum thickness of 2 km) and shifted close to the Alboran Channel. Two thin bodies of 0.03 SI magnetic susceptibility are located in the South Alboran Basin.

The MSB07 model (Fig. 6) represents the corner between the NE-SW and NW-SE dipole lineations. In this model, the deep body of 0.07 SI magnetic susceptibility shows a length of 40 km and a thickness of 5 km, in the southern part, while its thickness decreases toward the north. This body is located at 8–13 km of depth under the boundary of the East Alboran Basin. There are two thin 0.03 SI magnetic susceptibility bodies that are located beneath the sediments of the South Alboran Basin.

In the easternmost Alboran Sea, the SONOTRACH_S1 model (Fig. 7) reveals the origin of the NW-SE discontinuous anomaly. At that location, a deep body of 0.07 SI magnetic susceptibility is recognized, roughly 35 km wide, 4 km thick and with a depth of 7–11 km. Moreover, a 4 km thick body underlying the sediments of the Yusuf Basin and characterized by a 0.045 SI magnetic susceptibility is needed in order to fit the model (Fig. 7).

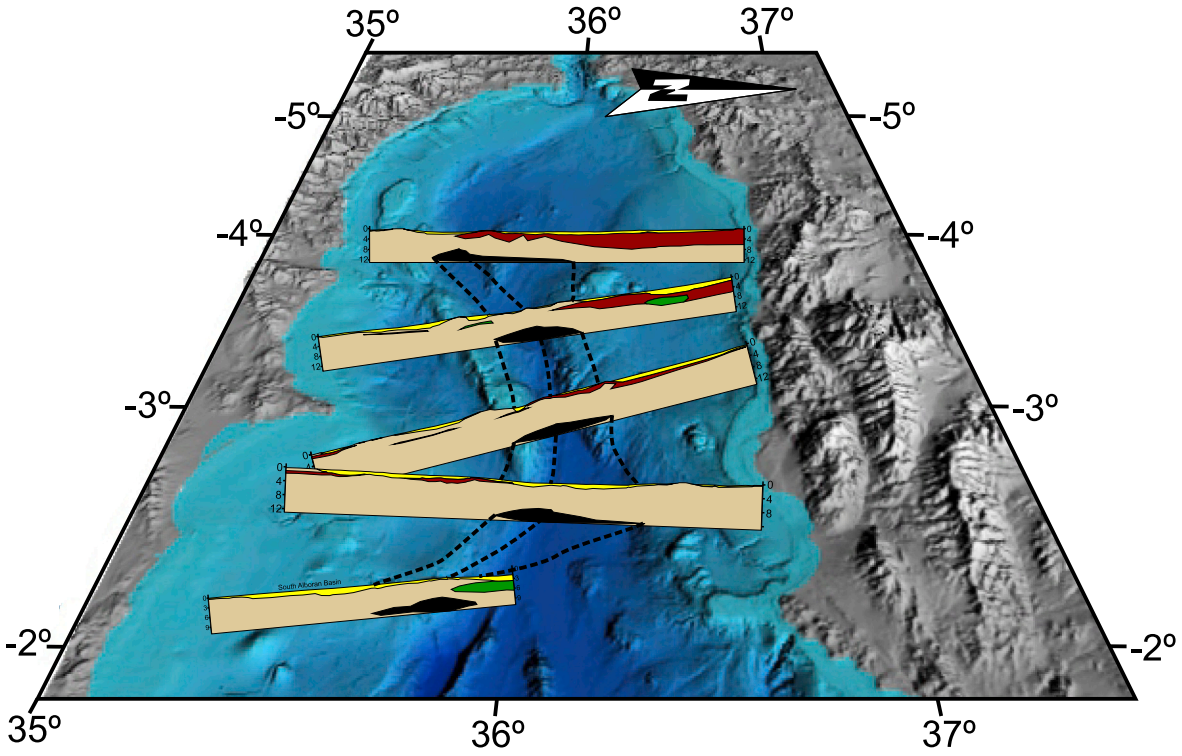

Fig. 8. Integration of cross sections of the causative body of the NE-SW and NW-SE magnetic anomaly lineations on the bathymetric map of the Alboran Sea. The color legend used are the same as those of the previous figures.

5. Discussion

5.1. New insights on the geometry and nature of the crustal igneous bodies

The magnetic forward models provide new insights on the geometry and nature of the crustal igneous bodies that are associated with magnetic dipoles. The intermediate to low magnetic susceptibility (0.02 to 0.04 SI) large size body is associated to secondary dipoles (less than 100 nT of amplitude). Even though the presence of this body is supported by the available data and the magnetic anomaly models, a detailed definition of its geometry would need higher magnetic resolution data that would account for the effect of local volcanic edifices. In any case, the models indicate that the body, which could be interpreted as a metamorphic layer with dispersed igneous rocks, should be extended over the northern part of the Alboran Sea, and locally in the southern part as well (Figs. 5, 6 and 8). According to the widespread presence of volcanic rocks (Fig. 1b) in this region of relatively thin continental crust (Galindo-Zaldivar et al., 1998), this metamorphic layer may be considered one of the sources of the eruptive rocks of the region, favored by crustal thinning (Hatzfeld, 1976; Suriñach and Vegas, 1993) and high heat flow (Andrés et al., 2018; Davies, 2013; Polyak et al., 1996). Conversely, on the southern Alboran Sea, the models reveal a more scattered presence of igneous bodies into the crust (Figs. 5, 6 and 7). Some of these bodies could be related to volcanic rocks, such as the low magnetic susceptibility bodies of the southern part of model TYRO91L17, and the SA2 dipole (Figs. 2 and 6). Other geometries for these low to medium susceptibility bodies are possible and require data with higher resolution. In any case, the contrast between the northern and southern Alboran Sea (Fig. 8), especially in the Malaga Basin, may also be interpreted as a sign of crustal differences (Alboran versus African domains), as some previous works pointed out (e.g., Booth-Rea et al., 2007; d'Acremont et al., 2020; de la Gómez Peña et al., 2020b). A special mention should be made of the Nador dipole (Figs. 1, 2 and 7) that highlights the deep connection between the Gourougou and Chafarinas volcanic edifices (Fig. 1) by a kilometric scale elongated *E*-W basic intrusion parallel to the African coast (Fig. 7). This deep basic intrusion cannot be related to surface structures, such as faults or folds, which are not E-W oriented (Fig. 1).

Regarding the group of magnetic dipoles without apparent links with the mapped igneous rocks, their attribution also needs to take into account the geological structures and evolution of the region. The magnetic dipoles P1 and P2 in the western Alboran Sea could be associated with peridotite bodies such as those identified onshore, given their symmetry with respect to the Gibraltar Arc (Fig. 2). These bodies could be similar to the outcropping ultrabasic massifs that are located in the western Internal Zones of the Betic and Rif cordilleras (Fig. 1, Garrido, 1995). The massifs (Ronda, Beni Bousera) have been correlated with magnetic anomalies in previous works (Amar et al., 2015; González-Castillo et al., 2015b). For example, in Amar et al. (2015) the anomaly related to the Beni Bousera peridotites is extended to the P2 dipole (note that the map displayed in Amar et al., 2015 shows the magnetic anomalies reduced to the pole, a type of processing that maximizes the highs and minimize the lows for positive magnetic susceptibilities).

The main NE-SW dipole lineation located in the central Alboran Sea has a trend parallel to the Alboran Ridge, which is mainly formed by volcanic rocks (Booth-Rea et al., 2007; Comas et al., 1999; Maestro--González et al., 2008; Polyak et al., 1996; Watts et al., 1993). The NE-SW aligned dipoles (Figs. 2 and 8), the analytic signal map (Fig. 3), and the forward models (Figs. 5 and 6) all evidence the presence of a single elongated body made of basic or intermediate igneous rocks. One possible interpretation of this model would involve considering the connection between the causative body of the dipole lineation and the volcanic highs, such as the Alboran Ridge. In this scenario, the body could be formed by a set of aligned magmatic chambers related to the volcanic rocks that are exposed on the surface, which are basic to intermediate composition and can have high magnetic susceptibility values (e.g., Duggen et al., 2008; Fernández-Soler et al., 2000). However, working against this interpretation is the fact that the center of the dipoles is not aligned with the volcanic highs, and that is the point where the bodies should be located. In some sectors, the centers of the dipoles are located north of the Alboran Ridge and of the Alboran Channel, instead (Figs. 5, 6 and 8). Moreover, a dipole has also been identified in the flat areas located at the western tip of the Eastern Alboran Basin (Figs. 2 and 6, model MSB07), suggesting a break in the correlation between causative body and volcanic high. Altogether, the results suggest no connection between the deep igneous body and the Alboran Ridge, or other outcropping igneous edifices, contrary to what proposed by Galdeano et al. (1974). In this setting, the Alboran Ridge could contain heterogeneous volcanic bodies smaller than 1 km, or thin

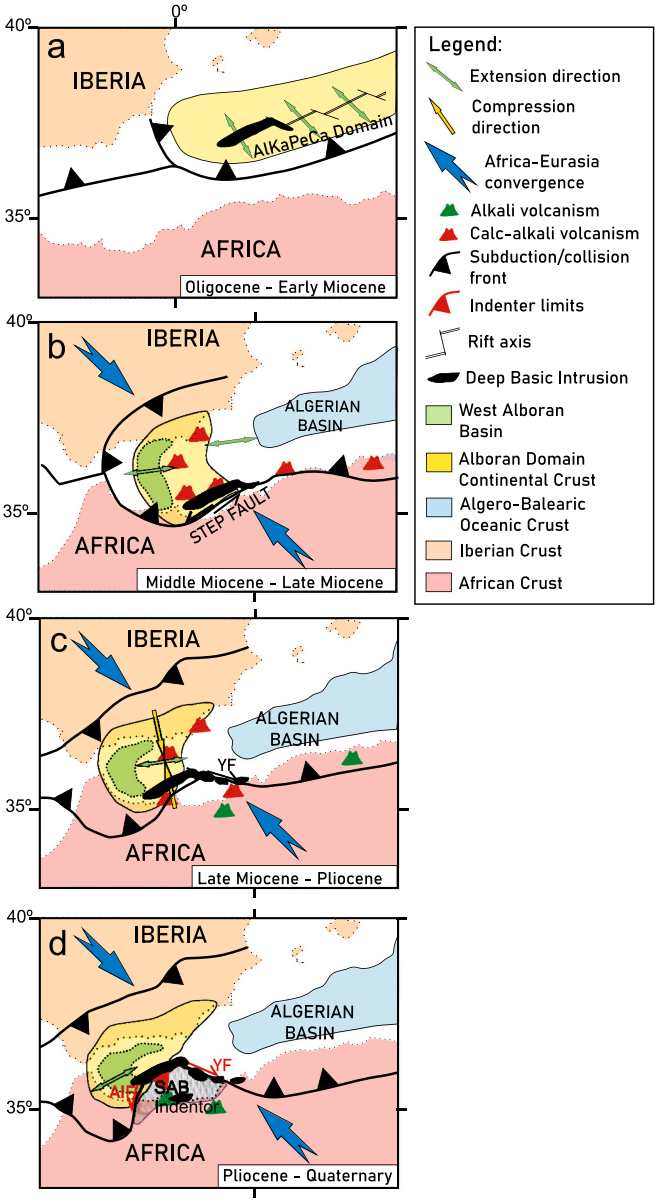

Fig. 9. Geodynamic evolution models based on the paleogeographic reconstructions of Do Couto et al. (2016) and Schettino and Turco (2011) and on the ages of volcanism of Duggen et al. (2005) and Maury et al. (2000). The limits of the tectonic indenter are from Estrada et al. (2018). AIF: Al Idrissi Fault, SAB: South Alboran Block, YF: Yusuf Fault. a. Model that considers the emplacement of the basic bodies during Oligocene-Early Miocene associated to the spreading axis of the Algerian basin. b. Model that considers the emplacement of the basic bodies during Middle-Miocene along the STEP fault.

volcanic layers interbedded with non-magnetic rocks, which would not cause relevant magnetic dipoles at a kilometric scale.-Go

An alternative interpretation would be to consider a magnetic mineralization as the causative body of the dipole lineations, similarly to what is observed in the Internal Zones of the Gibraltar Arc, where some iron mineralizations occur (e.g., Torres-Ruiz, 2006). However, the size of these deposits would be much smaller than the calculated size of the causative body associated with the dipole lineations observed in the Alboran Sea, even if a high susceptibility value is used to decrease the size of the modeled body.

The main NW-SE dipole lineation of the eastern Alboran Sea have roughly similar features to those of the NE-SW dipole lineation of the central Alboran Sea and those that continue along the Algerian coast (Fig. 2). Euler deconvolution depths are shallower and more scattered in the case of the NW-SE dipole lineation (Fig. 3). These anomalies are roughly located along the Yusuf fault system, including the Yusuf basin (Fig. 1b), and increase their irregularity eastwards, up to the smaller dipoles close to the Algerian coast (Fig. 2). This geometry points to a discontinuous aspect of the causative bodies, in contrast to the NE-SW continuous elongated body identified in the central Alboran Sea.

AS maxima are related to magnetization contrasts suggesting that deep basic igneous bodies are located along the northern African continental crust boundary (Figs. 1, 2 and 9), at the contact with the East Alboran Basin thinned crust and the Algerian oceanic crust (Booth-Rea et al., 2007; Do Couto et al., 2016; de la Gómez Peña et al., 2020a).

5.2. Geodynamic implications

The analysis of magnetic anomalies contributes to constrain the initial stages of the opening and evolution of the Alboran Sea (Fig. 9). The emplacement of the NE-SW and NW-SE dipole lineations must have occurred during the initial NNW-SSE extensional stages, based on their trend and disconnection from surface structures (Jolivet et al., 2021 and references therein). In fact, the NE-SW dipole lineation (Fig. 2) has a direction similar to the rift axis proposed in paleogeographic reconstructions of the AlKaPeCa Domain (Do Couto et al., 2016; Faccena et al., 2014; Mauffret et al., 2007; Schettino and Turco, 2011; Spakman et al., 2018). These bodies may have been the relict of the westwards rifting axis of the AlKAPeCa Domain that remained into the crust of the Alboran Domain (Fig. 9a, Bouillin et al., 1986; Mauffret et al., 2007; Romagny et al., 2020; Rosenbaum et al., 2002). Therefore, the age of emplacement of these deep basic bodies should be Oligocene to Lower Miocene. This extension was probably the result of the southward retreat of the slab attached to the African margin (Chertova et al., 2014; Do Couto et al., 2016; Faccena et al., 2014; Gueguen et al., 1997; Mauffret et al., 2007; Romagny et al., 2020; Rosenbaum et al., 2002; Schettino and Turco, 2011; Spakman et al., 2018). The magnetic anomalies that continue along the Algerian continental slope (Fig. 2) may also be a remnant of that rift, in agreement with the rift location proposed by Yelles et al. (2009).

After the Early Miocene, the extension changed direction to *E*-W, in response to the westward displacement of the Alboran Domain with orthogonal compression (Comas et al., 1992; Do Couto et al., 2016; Faccena et al., 2014; Mauffret et al., 2007; Rosenbaum et al., 2002; Royden, 1993). Magnetic, gravity and seismic reflection studies in the East Algerian basin show these two extensional stages (a NW-SE directed extension, followed by an E-W directed one) marked by an oceanic crust generation (Driussi et al., 2015).

In this scenario (Fig. 9b), the igneous bodies formed during the first extensional stage, along the rift and transfer fault axis, could have moved westward within the southern part of the Alboran Domain. During this period, the southern boundary of the Alboran Domain acted as a STEP fault that accommodated the westward displacement (Fig. 9b, d'Acremont et al., 2020). This period was marked by the generation of calk-alkaline magmatism (Middle Miocene to Late Pliocene) related to subduction processes and crustal contamination (Duggen et al., 2004, 2008; Fernández-Soler et al., 2000; Turner et al., 1999).

During post-Tortonian times, the westward retreat of the Gibraltar slab decreased its influence in this region, so the STEP fault activity also declined and the NW-SE compression increased its influence (d'Acremont et al., 2020; de la Gómez Peña et al., 2020b). The STEP fault was displaced northwards and deformed, which generated some of the modern faults of the Alboran Sea, such as the Yusuf fault (Fig. 9c, d'Acremont et al., 2020). The eastward change of orientation of the dipoles lineation to NW-SE and their heterogeneity may be due to the initial emplacement along a transform fault of the AlKaPeCa Domain rifting axis (Fig. 9a) and to a later fragmentation and disruption of the main body by the Yusuf fault (Fig. 9c, d). In addition, transtensional areas like the pull-apart Yusuf basin (Fig. 1b) may have favored the emplacement of new magmas (e.g., Cocchi et al., 2017; de la Gómez Peña et al., 2020b; Jolivet et al., 2021) that generated small dipoles into the main ones (Figs. 2, 7 SONOTRACH_S1 model). The emplacement of these igneous bodies could have determined the late evolution of the basins (Martínez-García et al., 2011). Later, this fault may have evolved into a boundary between the African continental crust and the Algerian oceanic crusts (Fig. 9d).

In recent times (Plio-Quaternary), the NE-SW elongated body acted as a rigid backstop block where the South Alboran Block collides (Fig. 9d). This contributed to the elevation of the Alboran Ridge (Estrada et al., 2018) and the development of conjugate strike-slip fault sets in the northern Alboran Sea. The indenter of the South Alboran Block is bounded by the Al Idrissi fault zone to the west (Estrada et al., 2018), which must be a very recent development (Pleistocene in age, Lafosse et al., 2020), since the western tip of the NW-SE anomaly lineation shows little displacement between the main dipoles (Fig. 2). To the east, the boundary of the indenter is the Yusuf fault, which forms a contact between the continental crust of the indenter and the magmatic crust of the East Alboran Basin (Figs. 1 and 9). Thus, the current northern position of the anomalies is conditioned by the NNW push of the indenter. The deep igneous intrusions condition the limit of the indenter and the deformation of the northern Alboran Sea.

5.2.1. Recent magmatism: The Nador dipole

The *E*-W orientation of the Nador dipole (Fig. 2) is not in line with the other major structures of the area and, consequently, it should be explained by the lithospheric evolution. We tentatively suggest that it may be connected to the emplacement of recent magmas related to the westward progression of the slab tear along the African margin (Fig. 9, Duggen et al., 2005; Hidas et al., 2019). While the Alboran Sea structures reached their current positions during the westward displacement of the Alboran domain, the subducted slab that generated the back-arc opening of the Algerian Basin was being decoupled from the African margin (Carminati et al., 1998; Chertova et al., 2014; Hidas et al., 2019; Jolivet et al., 2021). This process has also been proposed to explain the progression of the alkaline volcanism of the eastern Morocco and northern Algeria, as in the case of the Gourougou volcano (Duggen et al., 2005; Maury et al., 2000). Therefore, our hypothesis considers that the *E*-W elongate causative body of the Nador dipole is an intrusion generated by the last alkaline magmatism episode that affected eastern Morocco (Fig. 9d).

5.2.2. Implications for other marine basins

The analysis of the magnetic anomalies helps to explain the complex history of magmatism and deformations in the Alboran Sea. The results highlight the utility of potential field methods to improve the knowledge of deep igneous intrusions in marine basins. They also show the interaction between rifting intrusions with a STEP fault and the later tectonic indentation. Furthermore, they evidence that these rigid bodies condition the subsequent geodynamic evolution of marine basins. Literature shows examples of deep igneous intrusions in basins of other seas and oceans developed on thinned continental and transitional crust, such as the South China Sea (Li et al., 2008; Sun et al., 2014), the southern

Norwegian Sea (Planke et al., 2005), or the Bight basin, in southern Australia (Reynolds et al., 2017). Nevertheless, these igneous intrusions have frequently been considered as local features into the overall geodynamic of the basin. Our findings demonstrate that the interaction between magmatism and tectonic structures must be seriously considered, in order to fully understand the different geodynamic scenarios. This approach establishes a new framework for future studies that aim to decode the onset and tectonic evolution of marine basins.

6. Conclusions

The magnetic anomalies of the Alboran Sea reveal the location and structure of the main basic and intermediate igneous rock bodies that contribute to decipher the origin and evolution of the Alboran Sea basin.

The most relevant NE-SW and NW-SE dipole lineations that cross the Alboran Sea toward the Algerian basin are related to elongate basic or intermediate igneous intrusions with 4–6 km of thickness, and that are located at ~12 km of depth. These deep basic intrusions can represent the westward tip of the Oligocene-Miocene rifting of the AlKaPeCa Domain, related to the Algerian basin (Fig. 9a). These bodies were westward displaced, together with the Alboran Domain, and accommodated by a STEP fault in its southern boundary (Fig. 9b). The development, since the Late Miocene, of a tectonic indentation deformed the STEP fault which led to the development of the Yusuf fault. Then, transtensional processes occurring at the time when the STEP and Yusuf faults were active segmented the eastern part of the magmatic body (Fig. 9c). This development would have favored the emplacement of new magmas and contributed to the formation of the discontinuous NW-SE anomalies. During the post-Miocene compression (Fig. 9d), the former deep, rigid, basic rock bodies facilitated the development of the Alboran Ridge and the conspicuous strike-slip fault system associated to the tectonic indentation. Moreover, they reveal the scarce recent displacement of the left-lateral Al Idrissi fault and the reactivation of former crustal heterogeneities, such as the Yusuf fault.

The other major dipoles are associated with most of the volcanic edifices since the Middle-Late Miocene (e.g. Cabo de Gata, Djibouti Bank, Figs. 1 and 2). The most remarkable is the Nador dipole that connects the Gourougou and Chafarinas volcanoes offshore. Magnetic forward modeling of this dipole shows a 4 km thick, 60 km long *E*-W elongated body close to the coast line, at 5–9 km of depth. The E-W elongated crustal Nador dipole intrusion may be the consequence of the tearing of a subducting slab attached to the African margin.

Altogether, this makes the Alboran Sea an interesting example of tectonic inversion in oblique continental convergence and development of STEP faults, where the analysis of the magnetic anomalies helps to explain the complex history of magmatism and deformations. These results highlight the usefulness of potential field methods to improve the knowledge of deep igneous intrusions in other marine basins with thinned continental crusts.

Data availability

Magnetic dataset used in this article were obtained from the second version of the World Digital Magnetic Anomaly Map Project (http://wdmam.org/). Seismic profiles used in this article can be found at http://www.icm.csic.es/geo/gma/SurveyMaps, a dataset hosted at the Instituto de Ciencias del Mar, ICM-CSIC.

Declaration of Competing Interest

The authors declare that they have no known competing financial interests or personal relationships that could have appeared to influence the work reported in this paper.

Acknowledgements

The comments of two anonymous reviewers have improved the quality of this manuscript. This study was supported by projects CGL2016-80687-R AEI/FEDER, P18-RT-3275, B-RNM-301-UGR18 and RNM148 (Junta de Andalucía/FEDER). Y.M.M was supported by NASA under award number 80GSFC17M0002. V.T.S. was supported by the FPU PhD grant (16/04038). ICM-CSIC author acknowledges the Severo Ochoa funding from the Spanish government through the "Severo Ochoa Centre of Excellence" accreditation (CEX2019-000928-S). University of Granada supported this study by funding the APC for publishing as an Open Access articile through an agreement with Elsevier.

Appendix A. Supplementary data

Supplementary data to this article can be found online at https://doi.org/10.1016/j.margeo.2021.106696.

References

Amar, N., Khattach, D., Azdimousa, A., Chourak, M., Jabaloy, A., Manar, A., Amar, M., 2015. Structure and peridotite of Gibraltar arc southern bloc: gravimetric and aeromagnetic evidences. Arab. J. Geosci. 8 (11), 9801–9813.

Anahnah, F., Galindo-Zaldívar, J., Azzouz, O., Ruano, P., Chalouan, A., Pedrera, A., Bouregba, N., 2009. The Nador dipole: one of the main magnetic anomalies of the NE Rif. Trab. Geol. 29.

Andrés, J., Marzán, I., Ayarza, P., Martí, D., Palomeras, I., Torné, M., Carbonell, R., 2018. Curie point depth of the Iberian Peninsula and surrounding margins. A thermal and tectonic perspective of its evolution. J. Geophys. Res. Solid Earth 123 (3), 2049–2068.

Balanya, J.C., Crespo-Blanc, A., Díaz-Azpiroz, M., Expósito, I., Torcal, F., Pérez-Peña, V., Booth-Rea, G., 2012. Arc-parallel vs back-arc extension in the Western Gibraltar arc: Is the Gibraltar forearc still active? Geol. Acta 10 (3), 249–263.

Baratin, L.M., Mazzotti, S., Chéry, J., Vernant, P., Tahayt, A., Mourabit, T., 2016. Incipient mantle delamination, active tectonics and crustal thickening in Northern Morocco: Insights from gravity data and numerical modelling. Earth Planet. Sci. Lett. 454, 113–120.

Blanco, M.J., Spakman, W., 1993. The P-wave velocity structure of the mantle below the Iberian Peninsula: Evidence for subducted lithosphere below southern spain. Tectonophysics 221 (1), 13–34. https://doi.org/10.1016/0040-1951(93)90025-F.

Bohoyo, F., Galindo-Zaldívar, J., Maldonado, A., Schreider, A.A., Suriñach, E., 2002. Basin development subsequent to ridge-trench collision: the Jane Basin, Antarctica. Mar. Geophys. Res. 23 (5), 413–421.

Booth-Rea, G., Ranero, C.R., Martínez-Martínez, J.M., Grevemeyer, I., 2007. Crustal types and Tertiary tectonic evolution of the Alborán Sea, western Mediterranean. Geochem. Geophys. Geosyst. 8 (10).

Bouillin, J.P., Durand-Delga, M., Olivier, P., 1986. Betic-Rifian and Tyrrhenian arcs: distinctive features, genesis and development stages. In: Developments in Geotectonics, 21. Elsevier, pp. 281–304.

Carminati, E., Wortel, M.J.R., Meijer, P.T., Sabadini, R., 1998. The two-stage opening of the western–central Mediterranean basins: a forward modeling test to a new evolutionary model. Earth Planet. Sci. Lett. 160 (3–4), 667–679.

Catalán, M., Galindo-Zaldivar, J., Davila, J.M., Martos, Y.M., Maldonado, A., Gambôa, L., Schreider, A.A., 2013. Initial stages of oceanic spreading in the Bransfield Rift from magnetic and gravity data analysis. Tectonophysics 585, 102–112.

Catalán, M., Dyment, J., Choi, Y., Hamoudi, M., Lesur, V., Thebault, E., de Santis, A., Ishihara, T., Korhonen, J., Litvinova, T., Luis, J., Meyer, B., Milligan, P., Nakanishi, M., Okuma, S., Pilkington, M., Purucker, M., Ravat, D., Gaina, C., Maus, S., Quesnel, Y., Saltus, R., Taylor, P., 2016. Making a better magnetic map. Eos 97. https://doi.org/10.1029/2016EO054645.

Chertova, M.V., Spakman, W., Van den Berg, A.P., Van Hinsbergen, D.J.J., 2014. Absolute plate motions and regional subduction evolution. Geochem. Geophys. Geosyst. 15 (10), 3780–3792.

Cocchi, L., Passaro, S., Tontini, F.C., Ventura, G., 2017. Volcanism in slab tear faults is larger than in island-arcs and back-arcs. Nat. Commun. 8 (1), 1–12.

Comas, M.C., García-Dueñas, V., Jurado, M.J., 1992. Neogene tectonic evolution of the Alboran Sea from MCS data. Geo-Marine Lett. 12, 157–164.

Comas, M.C., Platt, J.P., Soto, J.I., Watts, A.B., 1999. 44. The origin and tectonic history of the Alboran Basin: insights from Leg 161 results. In: Proceedings of the Ocean Drilling Program Scientific Results, 161, pp. 555–580.

Corsini, M., Chalouan, A., Galindo-Zaldivar, J., 2014. Geodynamics of the Gibraltar Arc and the Alboran Sea region. J. Geodyn. 77, 1–3. https://doi.org/10.1016/j.jog.2014.04.005.

Coulon, C., Megartsi, M.H., Fourcade, S., Maury, R.C., Bellon, H., Louni-Hacini, A., Hermitte, D., 2002. Post-collisional transition from calc-alkaline to alkaline volcanism during the Neogene in Oranie (Algeria): magmatic expression of a slab breakoff. Lithos 62 (3-4), 87–110.

d'Acremont, E., Lafosse, M., Rabaute, A., Teurquety, G., Do Couto, D., Ercilla, G., Juan, C., Lépinay, M.B., Lafuerza, S., Galindo-Zaldivar, J., Estrada, F., Vazquez, J.T., Leroy, S., Poort, J., Ammar, A., Gorini, C., 2020. Polyphase tectonic evolution of

fore-arc basin related to STEP fault as revealed by seismic reflection data from the Alboran Sea (W-Mediterranean). Tectonics 39 (3). https://doi.org/10.1029/2019TC005885 e2019TC005885.
Davies, J.H., 2013. Global map of solid Earth surface heat flow. Geochem. Geophys. Geosyst. 14 (10), 4608–4622.
de la Gómez Peña, L., Grevemeyer, I., Kopp, H., Díaz, J., Gallart, J., Booth-Rea, G., Ranero, R.C., 2020a. a. The lithospheric structure of the Gibraltar Arc System from wide-angle seismic data. J. Geophys. Res. Solid Earth *125* (9) (e2020JB019854).
de la Gómez Peña, L., Ranero, C.R., Gràcia, E., Booth-Rea, G., 2020b. b. The evolution of the westernmost Mediterranean basins. Earth Sci. Rev. 103445. https://doi.org/10.1016/j.earscirev.2020.103445.
DeMets, C., Gordon, R.G., Argus, D.F., 2010. Geologically current plate motions. Geophys. J. Int. 181 (1), 1–80. https://doi.org/10.1111/j.1365-246X.2009.04491.x.
Do Couto, D., Gorini, C., Jolivet, L., Lebret, N., Augier, R., Gumiaux, C., d'Acremont, E., Ammar, A., Jabour, H., Auxietre, J.L., 2016. Tectonic and stratigraphic evolution of the Western Alboran Sea Basin in the last 25 Myrs. Tectonophysics 677-678, 280–311.
Doglioni, C., 1991. A proposal of kinematic modeling for W-dipping subduction possible application to the TyrrhenianeApennine system. Terra Nova 3, 423–434. https://doi.org/10.1111/j.1365-3121.1991. tb00172.x.
Driussi, O., Briais, A., Maillard, A., 2015. Evidence for transform motion along the South Balearic margin and implications for the kinematics of opening of the Algerian basin. Bull. Soc. Géol. France 186 (4-5), 353–370.
Duggen, S., Hoernle, K., Bogaard, P., Harris, C., 2004. Magmatic evolution of the Alboran Region: the role of subduction in forming the western Mediterranean and causing the Messinian Salinity Crisis. Earth Planet. Sci. Lett. 218, 91–108.
Duggen, S., Hoernle, K., van den Bogaard, P., Garbe-Schönberg, D., 2005. Post-collisional transition from subduction-to intraplate-type magmatism in the westernmost Mediterranean: evidence for continental-edge delamination of subcontinental lithosphere. J. Petrol. 46 (6), 1155–1201.
Duggen, S., Hoernle, K., Klügel, A., Geldmacher, J., Thirlwall, M., Hauff, F., Oates, N., 2008. Geochemical zonation of the Miocene Alborán Basin volcanism (westernmost Mediterranean): geodynamic implications. Contrib. Mineral. Petrol. 156 (5), 577.
El Bakkali, S., Gourgaud, A., Bourdier, J.L., Bellon, H., Gundogdu, N., 1998. Post-collision neogene volcanism of the Eastern Rif (Morocco): magmatic evolution through time. Lithos 45 (1–4), 523–543.
Estrada, F., Galindo-Zaldivar, J., Vázquez, J.T., Ercilla, G., D'Acremont, E., Alonso, B., Gorini, C., 2018. Tectonic indentation in the central Alboran Sea (westernmost Mediterranean). Terra Nova 30 (1), 24–33. https://doi.org/10.1111/ter.12304.
Faccena, C., Becker, T.W., Auer, L., Billi, A., Boschi, L., Brun, J.P., Capitanio, F.A., Funiciello, F., Horvàth, F., Jolivet, L., Piromallo, C., Royden, L., Rossetti, F., Serpelloni, E., 2014. Mantle dynamics in the Mediterranean. Rev. Geophys. 52, 283–332. https://doi.org/10.1002/2013RG000444.
Fernández-Soler, J., Martínez-Ruíz, F., Akhmanov, G., Akhmetzhanov, A., Stadnitskaya, A., Kozlova, E., Sautkin, A., Mazurenko, L., Ovsyannikov, D., Sadekov, A., Belenkaya, I., Suslova, E., Goncharov, D., 2000. Bottom sampling. In: Kenyon, N.H., Ivanov, M.K., Azhmetzhanov, A.M., Akhmanov, G.G. (Eds.), Multidisciplinary Study of Geological Processes on the North East Atlantic and Western Mediterranean Margins, Preliminary Results of Geological and Geophysical Investigations During the TTR-9 of R/V Professor Logachev, June- July, 1999, 56. IOC Technical Series, UNESCO, pp. 85–91.
Galdeano, A., Courtillot, V., Le Borgne, E., Le Mouel, J.L., Rossignol, J.C., 1974. An aeromagnetic survey of the southwest of the western Mediterranean: Description and tectonic implications. Earth Planet. Sci. Lett. 23, 323–336.
Galindo-Zaldivar, J., González-Lodeiro, F., Jabaloy, A., Maldonado, A., Schreider, A.A., 1998. Models of magnetic and Bouguer gravity anomalies for the deep structure of the central Alboran Sea basin. Geo-Mar. Lett. 18, 10–18.
Garcia-Castellanos, D., Villaseñor, A., 2011. Messinian salinity crisis regulated by competing tectonics and erosion at the Gibraltar arc. Nature 480 (7377), 359–363.
García-Dueñas, V., Balanyá, J.C., Martínez-Martínez, J.M., 1992. Miocene extensional detachments in the outcropping basement of the Northern Alboran Basin (Betics) and their tectonic implications. Geo-Mar. Lett. 12, 88–95.
Garrido, C.J., 1995. Estudio Geoquimico de las Capas Maficas del Macizo Ultramafico de Ronda (Cordillera Betica, Espana). Doctoral dissertation. Universidad de Granada.
Gill, R.C.O., Aparicio, A., El Azzouzi, M., Hernandez, J., Thirlwall, M.F., Bourgois, J., Marriner, G.F., 2004. Depleted arc volcanism in the Alboran Sea and shoshonitic volcanism in Morocco: geochemical and isotopic constraints on Neogene tectonic processes. Lithos 78 (4), 363–388.
González-Castillo, L., Galindo-Zaldivar, J., de Lacy, M.C., Borque, M.J., Martinez-Moreno, F.J., García-Armenteros, J.A., Gil, A.J., 2015a. a. Active rollback in the Gibraltar Arc: Evidences from CGPS data in the western Betic Cordillera. Tectonophysics 663, 310–321.
González-Castillo, L., Galindo-Zaldívar, J., Junge, A., Martínez-Moreno, F.J., Löwer, A., de Galdeano, C.S., Martínez-Martos, M., 2015b. b. Evidence of a large deep conductive body within the basement of the Guadalquivir foreland Basin (Betic Cordillera, S-Spain) from tipper vector modelling: Tectonic implications. Tectonophysics 663, 354–363.
Govers, R., Wortel, M.J.R., 2005. Lithosphere tearing at STEP faults: Response to edges of subduction zones. Earth Planet. Sci. Lett. 236 (1–2), 505–523.
Gueguen, E., Doglioni, C., Fernandez, M., 1997. Lithospheric boudinage in the Western Mediterranean back-arc basin. Terra Nova 9 (4), 184–187.
Gueguen, E., Doglioni, C., Fernandez, M., 1998. On the post-25 Ma geodynamic evolution of the western Mediterranean. Tectonophysics 298 (1-3), 259–269. https://doi.org/10.1016/S0040-1951(98)00189-9.
Gutscher, M.A., Dominguez, S., Westbrook, G.K., Le Roy, P., Rosas, F., Duarte, J.C., Sallarès, V., 2012. The Gibraltar subduction: A decade of new geophysical data. Tectonophysics 574, 72–91.
Hatzfeld, D., 1976. Étude sismologique et gravimétrique de la estructure profonde de la mer d'Alborán: Mise en évidence d'un manteau anormal. C. R. Acad. Sci. Ser. IIA Earth Planet. Sci. 5, 483–500.
Heuret, A., Lallemand, S., 2005. Plate motions, slab dynamics and back-arc deformation. Phys. Earth Planet. Inter. 149 (1-2), 31–51.
Hidas, K., Garrido, C.J., Booth-Rea, G., Marchesi, C., Bodinier, J.L., Dautria, J.M., Azzouni-Sekkal, A., 2019. Lithosphere tearing along STEP faults and synkinematic formation of lherzolite and wehrlite in the shallow subcontinental mantle. Solid Earth 10 (4), 1099–1121.
Hoernle, K., Bogaard, P., Duggen, S., Mocek, B., Garbe-Schönberg, D., 1999. Evidence for Miocene subduction beneath the Alboran Sea: $^{40}Ar/^{39}Ar$ dating and geochemistry of volcanic rocks from Holes 977A and 978A. In: Zahn, R., Comas, M.C., Klaus, A. (Eds.), Proceedings of the Ocean Drilling Program, Scientific Results, 161, pp. 357–373.
Jolivet, L., Menant, A., Roche, V., Le Pourhiet, L., Maillard, A., Augier, R., Canva, A., 2021. Transfer zones in Mediterranean back-arc regions and tear faults. BSGF-Earth Sci. Bull. 192 (1), 11.
Juan, C., Ercilla, G., Hernández-Molina, J.F., Estrada, F., Alonso, B., Casas, D., García, M., Farrán, M., Llave, E., Palomino, D., Vázquez, J.T., Medialdea, T., Gorini, C., d'Acremont, E., El Moumni, B., Ammar, A., 2016. Seismic evidence of current-controlled sedimentation in the Alboran Sea during the Pliocene and Quaternary: Palaeoceanographic implications. Mar. Geol. 378, 292–311. https://doi.org/10.1016/j.margeo.2016.01.006.
Keating, P., Sailhac, P., 2004. Use of the analytical signal to identify magnetic anomalies due to kimberlite pipes. Geophysics 69, 180–190.
Lafosse, M., d'Acremont, E., Rabaute, A., Estrada, F., Jollivet-Castelot, M., Vazquez, J.T., Galindo-Zaldivar, J., Ercilla, G., Alonso, B., Smit, J., Ammar, A., Gorini, C., 2020. Plio-Quaternary tectonic evolution of the southern margin of the Alboran Basin (Western Mediterranean). Solid Earth 11 (2), 741–765. https://doi.org/10.5194/se-11-741-2020.
Lawver, L.A., Hawkins, J.W., 1978. Diffuse magnetic anomalies in marginal basins: Their possible tectonic and petrologic significance. Tectonophysics 45 (4), 323–339.
Lesur, V., Hamoudi, M., Choi, Y., Dyment, J., Thébault, E., 2016. Building the second version of the world digital magnetic anomaly map (WDMAM). Earth Planets Space 68 (1), 1–13.
Li, C.F., Zhou, Z., Li, J., Chen, B., Geng, J., 2008. Magnetic zoning and seismic structure of the South China Sea ocean basin. Mar. Geophys. Res. 29 (4), 223–238.
Li, C.F., Lu, Y., Wang, J., 2017. A global reference model of Curie-point depths based on EMAG2. Sci. Rep. 7, 45129.
Maestro-González, A., Bárcenas, P., Vázquez, J.T., Díaz-del-Río, V., 2008. The role of basement inheritance faults in the recent fracture system of the inner shelf around Alboran Island, Western Mediterranean. Geo-Marine Letters 28 (1), 53–64. https://doi.org/10.1007/s00367-007-0089-8.
Malinverno, A., Ryan, W.B., 1986. Extension in the Tyrrhenian Sea and shortening in the Apennines as result of arc migration driven by sinking of the lithosphere. Tectonics 5 (2), 227–245.
Mancilla, F.D.L., Stich, D., Berrocoso, M., Martín, R., Morales, J., Fernandez-Ros, A., Páez, R., Pérez-Peña, A., 2013. Delamination in the Betic Range: Deep structure, seismicity, and GPS motion. Geology 41 (3), 307–310. https://doi.org/10.1130/G33733.1.
Martínez-García, P., Soto, J.I., Comas, M., 2011. Recent structures in the Alboran Ridge and Yusuf fault zones based on swath bathymetry and sub-bottom profiling: evidence of active tectonics. Geo-Mar. Lett. 31 (1), 19–36.
Mauffret, A., Ammar, A., Gorini, C., Jabour, H., 2007. The Alboran Sea (Western Mediterranean) revisited with a view from the Moroccan margin. Terra Nova 19 (3), 195–203.
Maury, R.C., Fourcade, S., Coulon, C., Bellon, H., Coutelle, A., Ouabadi, A., Réhault, J.P., 2000. Post-collisional Neogene magmatism of the Mediterranean Maghreb margin: a consequence of slab breakoff. C. R. Acad. Sci. Ser. IIA-Earth Planet. Sci. 331 (3), 159–173.
Nabighian, M.N., 1984. Toward a three-dimensional automatic interpretation of potential field data via generalized Hilbert transforms: fundamental relations. Geophysics 49 (6), 780–786.
Neres, M., Carafa, M.M.C., Fernandes, R.M.S., Matias, L., Duarte, J.C., Barba, S., Terrinha, P., 2016. Lithospheric deformation in the Africa-Iberia plate boundary: Improved neotectonic modeling testing a basal-driven Alboran plate. J. Geophys. Res. Solid Earth 121 (9), 6566–6596. https://doi.org/10.1002/2016JB013012.
Pedley, R.C., Busby, J.P., Dabek, Z.K., 1993. GRAVMAG user manual–interactive 2.5 D gravity and magnetic modelling. In: British Geological Survey, Technical Report WK/93/26/R. 73.
Planke, S., Rasmussen, T., Rey, S.S., Myklebust, R., 2005. Seismic characteristics and distribution of volcanic intrusions and hydrothermal vent complexes in the Vøring and Møre basins. In: Geological Society, London, Petroleum Geology Conference Series, 6. Geological Society of London, pp. 833–844. No. 1. January.
Polyak, B.G., Fernàndez, M., Khutorskoy, M.D., Soto, J.I., Basov, I.A., Comas, M.C., Khain, V.Y., Alonso, B., Agapova, G.V., Mazurova, I.S., Negredo, A., Tochitsky, V.O., de la Linde, J., Bogdanov, N.A., Banda, E., 1996. Heat flow in the Alboran Sea, westrn Mediterranean. Tectonophysics 263, 191–218.
Quesnel, Y., Catalán, M., Ishihara, T., 2009. A new global marine magnetic anomaly data set. J. Geophys. Res. Solid Earth 114 (B4).
Ravat, D., 1996. Analysis of the Euler method and its applicability in environmental magnetic investigations. J. Environ. Eng. Geophys. 229–238.

Reid, A.B., Allsop, J.M., Granser, H., Millet, A.J., Somerton, L.W., 1990. Magnetic interpretation in three dimensions using the Euler deconvolution. Geophysics 55 (1), 80–91.
Reynolds, P., Holford, S., Schofield, N., Ross, A., 2017. The shallow depth emplacement of mafic intrusions on a magma-poor rifted margin: an example from the Bight Basin, southern Australia. Mar. Pet. Geol. 88, 605–616.
Roest, W.R., Pilkington, M., 1993. Identifying remanent magnetization effects in magnetic data. Geophysics 58, 653–659.
Roest, W.R., Verhoef, J., Pilkington, M., 1992. Magnetic interpretation using the 3-D analytical signal. Geophysics 57, 116–125.
Romagny, A., Jolivet, L., Menant, A., Bessière, E., Maillard, A., Canva, A., Augier, R., 2020. Detailed tectonic reconstructions of the Western Mediterranean region for the last 35 Ma, insights on driving mechanismsReconstructions détaillées de la Méditerranée occidentale depuis 35 Ma, implications en terme de mécanismes moteur. Bull. Soc. Géol. France 191 (1).
Rosenbaum, G., Lister, G.S., Duboz, C., 2002. Reconstruction of the tectonic evolution of the western Mediterranean since the Oligocene. J. Virtual Explor. 8, 107–130.
Royden, L.H., 1993. Evolution of retreating subduction boundaries formed during continental collision. Tectonics 12 (3), 629–638.
Salem, A., Ravat, D., Gamey, T.J., Ushjima, K., 2002. Analytical signal approach and its applicability in environmental magnetic investigations. J. Appl. Geophys. 49, 231–244.
Schettino, A., Turco, E., 2011. Tectonic history of the western Tethys since the Late Triassic. Bulletin 123 (1-2), 89–105.
Seber, D., Barazangi, M., Ibenbrahim, A., Demnati, A., 1996. Geophysical evidence for lithospheric delamination beneath the Alboran Sea and Rif–Betic mountains. Nature 379 (6568), 785–790.
Spakman, W., Wortel, R., 2004. A tomographic view on western Mediterranean geodynamics. In: The TRANSMED Atlas. The Mediterranean Region from Crust to Mantle. Springer, Berlin, Heidelberg, pp. 31–52.
Spakman, W., Chertova, M.V., van den Berg, A., van Hinsbergen, D.J., 2018. Puzzling features of western Mediterranean tectonics explained by slab dragging. Nat. Geosci. 11 (3), 211–216. https://doi.org/10.1038/s41561-018-0066-z.
Sun, Q., Wu, S., Cartwright, J., Wang, S., Lu, Y., Chen, D., Dong, D., 2014. Neogene igneous intrusions in the northern South China Sea: Evidence from high-resolution three dimensional seismic data. Mar. Pet. Geol. 54, 83–95.
Suriñach, E., Vegas, R., 1993. Estructura general de la corteza en una transversal del Mar de Alborán a partir de datos de sísmica de refracción-reflexión de gran ángulo. Interpretación geodinámica. Geogaceta 14, 126–128.
Taylor, B. (Ed.), 2013. Backarc Basins: Tectonics and Magmatism. Springer Science & Business Media.
Taylor, B., Zellmer, K., Martinez, F., Goodliffe, A., 1996. Sea-floor spreading in the Lau back-arc basin. Earth Planet. Sci. Lett. 144 (1), 35–40.
Telford, W.M., Geldart, L.P., Sheriff, R.E., Sheriff, R.E., 1990. Applied Geophysics. Cambridge university press.
Thomson, D.T., 1982. EULDPH: A new technique for making computer-assisted depth estimates from magnetic data. Geophysics 55, 80–91.
Torres-Ruiz, J., 2006. Geochemical constraints on the genesis of the Marquesado iron ore deposits, Betic Cordillera, Spain: REE, C, O, and Sr isotope data. Econ. Geol. 101 (3), 667–677.
Turner, S.P., Platt, J.P., George, R.M.M., Kelley, S.P., Pearson, D.G., Nowell, G.M., 1999. Magmatism associated with orogenic collapse of the Betic–Alboran domain, SE Spain. J. Petrol. 40 (6), 1011–1036.
Valera, J.L., Negredo, A.M., Villaseñor, A., 2008. Asymmetric delamination and convective removal numerical modeling: comparison with evolutionary models for the Alboran Sea region. In: Earth Sciences and Mathematics. Birkhäuser Basel, pp. 1683–1706.
Watts, A.B., Platt, J.P., Buhl, P., 1993. Tectonic evolution of the Alboran Sea basin. Basin Res. 5, 153–177.
Weissel, J.K., 1981. Magnetic lineations in marginal basins of the western Pacific. Philos. Trans. Royal Soc. Lond. Ser. A Math. Phys. Sci. 300 (1454), 223–247.
Yelles, A., Domzig, A., Déverchère, J., Bracène, R., de Lépinay, B.M., Strzerzynski, P., Djellit, H., 2009. Plio-Quaternary reactivation of the Neogene margin off NW Algiers, Algeria: the Khayr al Din bank. Tectonophysics 475 (1), 98–116.
Zeck, H.P., Kristensen, A.B., Williams, I.S., 1998. Post-collisional volcanism in a sinking slab setting—crustal anatectic origin of pyroxene–andesite magma, Caldear volcanic province, southeastern Spain. Lithos 45, 499–522.